

Article

Geochemical Assessment of Potential Sources for Nitrate in the Wasia Aquifer, Al Kharj Area, Central Saudi Arabia

Abid Khogali ^{1,*}, Peter Birkle ², Abdulaziz Al-Shaibani ^{1,3}, Martin Keller ^{3,4},
Bassam Tawabini ¹ and Mohammad Makkawi ¹

¹ Geosciences Department, College of Petroleum Engineering and Geosciences, King Fahd University of Petroleum & Minerals, Dhahran 31261, Saudi Arabia; shaibani@kfupm.edu.sa (A.A.-S.); bassamst@kfupm.edu.sa (B.T.); makkawi@kfupm.edu.sa (M.M.)

² Geology Technology Team, EXPEC Advanced Research Center (EXPEC ARC), Saudi Aramco, Dhahran 31311, Saudi Arabia; peter.birkle@aramco.com

³ Ministry of Environment, Water, and Agriculture, Riyadh 11195, Saudi Arabia; martin.keller@fau.de

⁴ GeoZentrum Nordbayern, Universität Erlangen, Schlossgarten 5, 91054 Erlangen, Germany

* Correspondence: g201605760@kfupm.edu.sa; Tel.: +966-59-4900753

Received: 1 April 2020; Accepted: 10 May 2020; Published: 22 May 2020



Abstract: Nitrate (NO_3^-) represents one of the major groundwater constituents with increasing distribution and concentration in the Kingdom of Saudi Arabia. This study aimed to determine potential sources of nitrate in the Early to Late Cretaceous Wasia aquifer system at the Al Kharj area (Central Saudi Arabia) by an integrative approach using groundwater geochemistry, nitrate isotopes ($^{15}\text{N}\text{-NO}_3$ and $^{18}\text{O}\text{-NO}_3$), and tritium (^3H) measurements. The lowest saline groundwater samples (TDS = 1400–2000 mg/L) from the peripheral zone were representative for pristine groundwater from the Wasia aquifer with nitrate concentrations below 20 mg/L and low $^{18}\text{O}\text{-NO}_3$ ratios (8.7–20.6‰) but enriched $^{15}\text{N}\text{-NO}_3$ values (up to 10.8‰). In contrast, 11 out of 34 analyzed water samples from irrigation wells and cattle watering wells exceeded the World Health Organization (WHO) drinking water guideline value for nitrate of 50 mg/L with maximum concentrations of up to 395 mg/L. Nitrate fertilizers and atmospheric deposition are the main sources of nitrate in groundwater in the eastern and northern sections of the study area. The combination of elevated salinities (4940–7330 mg/L), NO_3 (111–395 mg/L), boron (516–1430 $\mu\text{g/L}$), and enriched $^{18}\text{O}\text{-NO}_3$ (21.7–25.8‰) ratios with depleted $^{15}\text{N}\text{-NO}_3$ (5.7–7.6‰) confirm the local influx of evaporated irrigation water with remnants of dissolved fertilizer into the Wasia groundwater system. There was no evidence for the influx of animal or human wastes from adjacent dairy, poultry, and housing infrastructures. Tritium concentrations below the detection limit of 0.8 TU for most borehole samples implied the absence of recent natural recharge. The estimated annual average N influx of 3.34 to 6.67 kg/ha to the Wasia aquifer requires a combination of atmospheric deposition and anthropogenic sources (mainly nitrate fertilizers) to increase the nitrogen content of the Wasia aquifer.

Keywords: Wasia aquifer; nitrate sources; stable isotopes; geochemistry

1. Introduction

The increasing enrichment of nitrate (NO_3^-) in groundwater by anthropogenic sources represents a worldwide problem for water quality standards [1–3]. Drinking water with elevated nitrate concentrations may cause severe health issues like blue-baby syndrome (methemoglobinemia) [3]. Multiple studies have been carried out regarding the occurrence and source of nitrate in aquifers [4–7]. High levels of nitrate in the subsurface are usually attributed to the use of inorganic fertilizers,

animal manure, airborne nitrogen, and non-agricultural sources such as lawn fertilizer, septic systems, and domestic animals in residential areas [8,9]. Natural sources, like atmospheric deposition, nitrogen releases from nitrogen-bearing bedrocks, and hydrothermal waters, are also possible sources of nitrogen [10].

Al Kharj city is one of the oldest agricultural regions in Saudi Arabia, as it falls within a graben system that is covered by fertile Quaternary superficial deposits. Below this Quaternary cover, the graben fill hosts the Biyadh aquifer and the overlying Wasia aquifer. The Wasia aquifer is one of the most prolific sources of groundwater in Saudi Arabia that provides freshwater resources for the city of Riyadh [11,12]. In the Al Kharj area, the Wasia aquifer is primarily exploited for agricultural purposes. It is estimated that more than 90% of the center pivots of the dairy farms and agricultural complexes are used to grow alfalfa.

Several studies have focused on the chemical characteristics of groundwater in the Al Kharj area [13–17]. Most of these studies have detected elevated nitrate concentrations in this area, which were assumed to be linked to agricultural activities. Some of the studied wells are remote from anthropogenic activities, which raises uncertainty about the source of nitrate in this aquifer. None of these studies have clearly assessed the sources and distribution of these elevated nitrate concentrations. Isotope-based approaches were successfully applied to identify the possible origins of nitrate [18,19]. The radioactive isotope tritium (^3H) can be employed to distinguish groundwater recharge during the pre-bomb time from younger water [4,20]. The tritium content in the atmosphere increased dramatically since the start of the subaerial testing of nuclear bombs in 1952. After 1963, the tritium rate in the atmosphere declined due to the fact of its radioactive decay, precipitation, and the termination of atmospheric nuclear testing. Tritium has a half-life of approximately 12.3 years and is usually expressed in tritium units (TU) [20,21]. The approximate residence time of groundwater is reconstructed by correlating the measured tritium concentrations with the atmospheric tritium decay curve since 1952.

In this study, hydrochemical (major, minor, and trace element) and isotopic ($^{15}\text{N}\text{-NO}_3$, $^{18}\text{O}\text{-NO}_3$) analysis on borehole samples from the shallow Wasia aquifer were performed to assess the potential sources and distribution of nitrate in the Al Kharj area. Isotopic fingerprints of tritium (^3H) were used to assess the possibility of recent recharge to the Wasia aquifer in the Al Kharj area. As a novelty to previous hydrogeological and geochemical studies, the combined assessment of hydrochemical data of major ions (Na, Ca, K, Mg, Cl, HCO_3 , SO_4 , NO_3) and minor elements (i.e., B, Fe), stable ($^{15}\text{N}\text{-NO}_3$, $^{18}\text{O}\text{-NO}_3$), and radiogenic isotopes (^3H) allows quantitative characterization of the pristine composition of the Wasia aquifer in the study area and to trace the source and migration of anthropogenic influx from the surface.

2. Background

2.1. Location and Geology

The study area is located east of Al Kharj city in Central Saudi Arabia, SE of Riyadh city. The area is situated between 24.00° N and 24.35° N latitude and 47.40° E and 48.00° E longitude on an altitude of 400 to 480 m above sea level (Figure 1). Wadi As-Sahba crosses the central part and represents the lowest elevation point in the study area [14]. The study area is dominated by arid climatic conditions with a wide range of temperatures from 48° C during summer to 3° C in the winter [14]. The evaporation rate reaches an annual level of 2000 mm, while the average annual rainfall is below 100 mm [22].

From the geological point of view, the Wasia Group represents an important succession within the extensive Cretaceous sequence of the Arabian Platform (Figure 2). In the study area, the clastic part of the Wasia Group consists of sandstone interbedded with shaly beds. The Albian to Turonian Wasia Group is unconformably underlain by the siliciclastic, Barremian Biyadh Formation, and unconformably covered by Santonian to Danian carbonates of the Aruma Group (Figure 2). The carbonates of the Early Eocene Umm Er Radhuma Formation (Figure 1B) unconformably lie above the Aruma Group. On a regional scale, the Wasia Group crops out as an intermittent curve-shaped structure

between latitudes of 18° N and 30° N, with a length and width of about 1500 km and 50 km, respectively (Figure 1) [23,24]. Outcrop thickness of the Group within this discontinuous arc varies from approximately 30 m in the south to almost 90 m in the north [24,25].

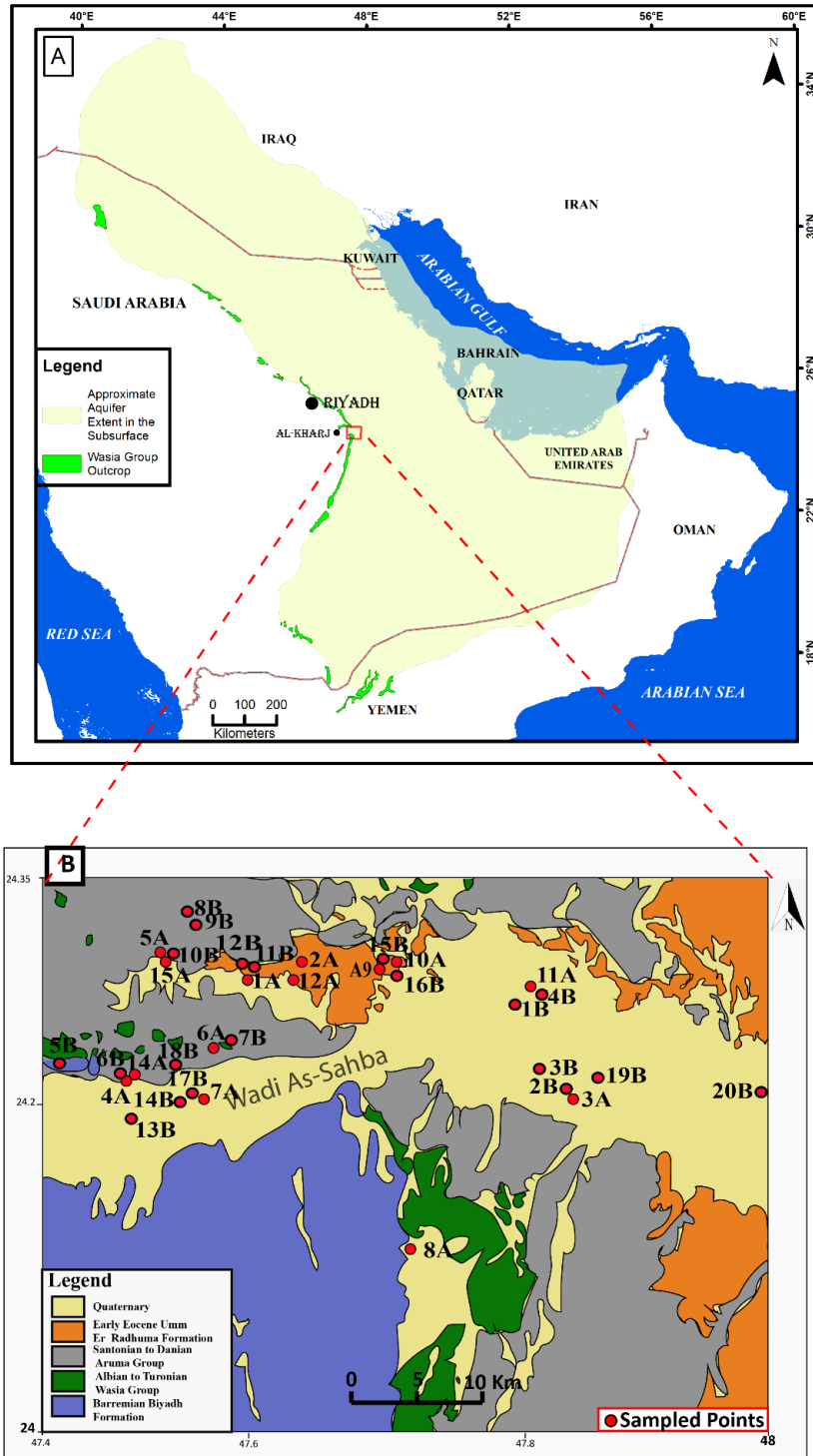


Figure 1. (A) A map of the Arabian Peninsula showing the location of the surface outcrop of the Cretaceous Wasia and the regional extent of the Wasia aquifer in the subsurface (modified from Reference [12,16]). (B) A geological map of the Al Kharj area in Central Saudi Arabia with sampling points of supply water wells from the present study. A wadi is a valley, ravine, or channel that is dry except in rainy season.

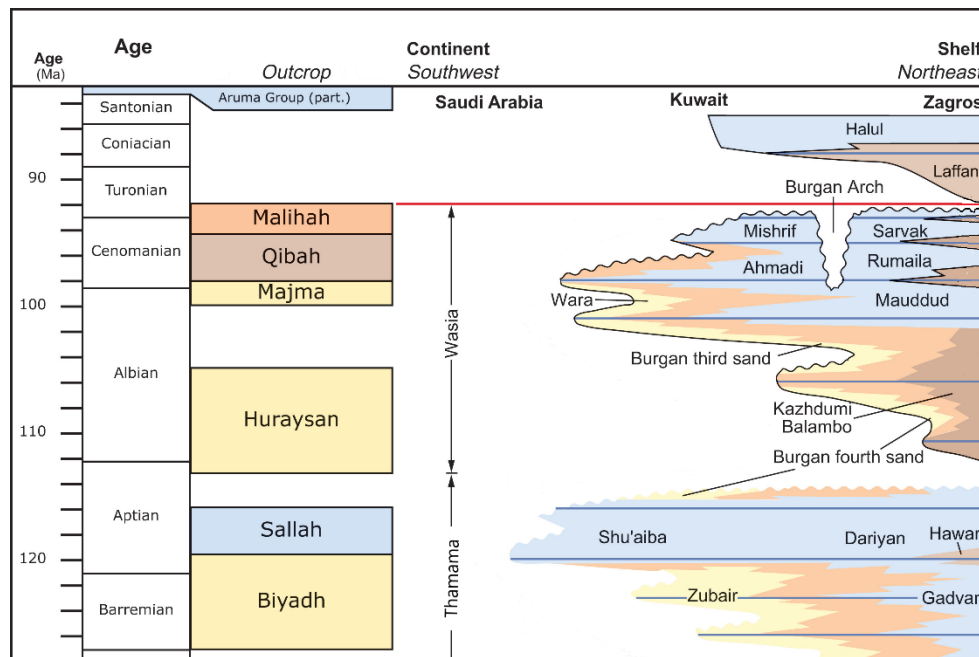


Figure 2. Stratigraphic chart of the Wasia Group and adjacent formations from the southwest to northeast of the Arabian Plate (modified from Reference [25]).

2.2. Hydrogeology

The main freshwater aquifer in the study area is composed of the Biyadh Formation of the Thamama Group and the Huraysan and Majma Formations of the Wasia Group (Figure 2). The intervening Sallah Formation of the Thamama Group is only a few meters thick and has similar hydraulic parameters to both the underlying and overlying aquifer components [25]. Piezometric heads of the Thamama Group and of the Wasia Group are indistinguishable in the study area. Most of the wells investigated partially penetrate the Wasia aquifer, while some of them were drilled through the Wasia strata into the Biyadh aquifer. Hence, for the purpose of this study, we will refer to this combined aquifer system as the Wasia aquifer or aquifer system.

The conceptual groundwater model (Figure 3) shows unconfined aquifers in the study area, while farther east, confined conditions prevail caused by increasingly shaly sediments acting as aquitards. Rain falls either on the outcrops of the aquifers or on a thin cover of Quaternary sediments, except for in the graben structure, where the Quaternary succession is thicker. While the vast majority of rainfall is lost to evapotranspiration, surface runoff is towards Wadi As-Sahba, where transmission losses routing downslope along the wadi add to groundwater recharge. Groundwater recharge through direct infiltration is very limited but has an additional component in irrigation return flow, the effect of which is the topic of this study. Except for evaporation [22], none of the components of the water balance has yet been specified for the Al Kharj area.

The Google Earth Map of the study area (Figure 4) shows an eastward decrease of the piezometric head from 340 m.a.s.l. to 270 m.a.s.l. (meters above the sea level) with the location of Al Kharj, the local wastewater treatment plant, and major agricultural irrigation zones (green to dark grey colored circles = center pivots). Groundwater flow lines (Figure 4) indicate that the major groundwater flow is directed eastward along Wadi As-Sahba coinciding with the general flow system of the Wasia–Biyadh aquifer system on a regional scale. However, with the migration of farms increasing in size and abstraction eastward along the wadi to the east, groundwater is successively drawn also from both flanks towards the wadi. Concomitantly, an elongated cone of depression is formed, and the eastern end is located just outside the study area. It is also in this area that the Shu'aiba aquitard starts to effectively separate the Biyadh from the Wasia aquifer (Figure 3). Similarly, the Lower Aruma aquitard

starts to separate the Wasia from the Aruma aquifer. In both cases, confined conditions are imposed on the aquifers and locally flowing wells are observed there.

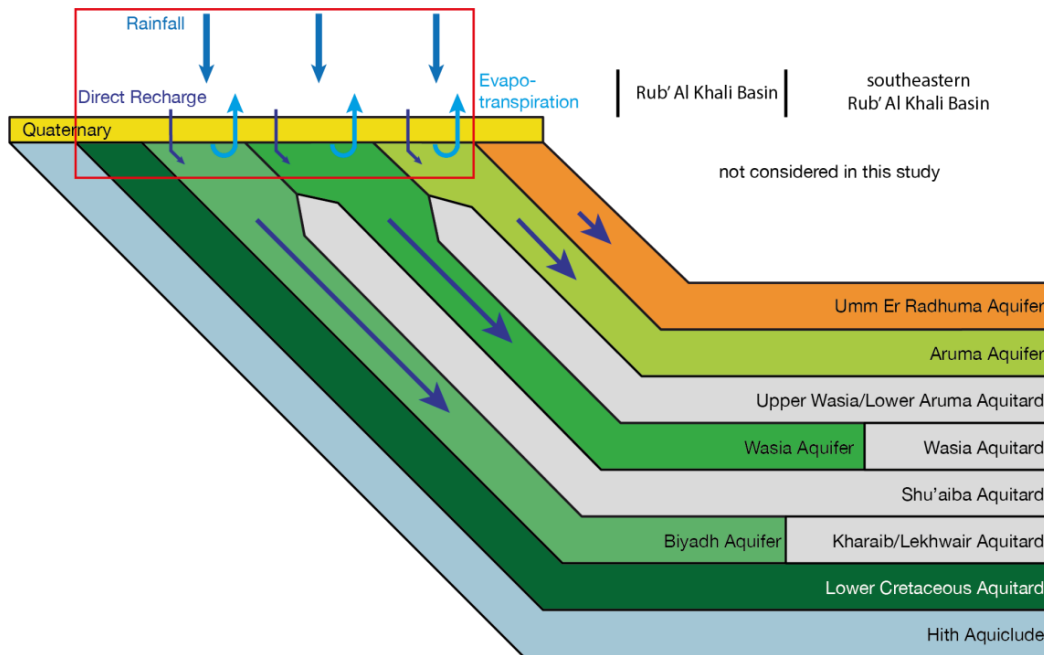


Figure 3. Conceptual aquifer model (not to scale) of the Al Kharj area (red box) with strata discussed in the text. Surface runoff is not shown in this figure.

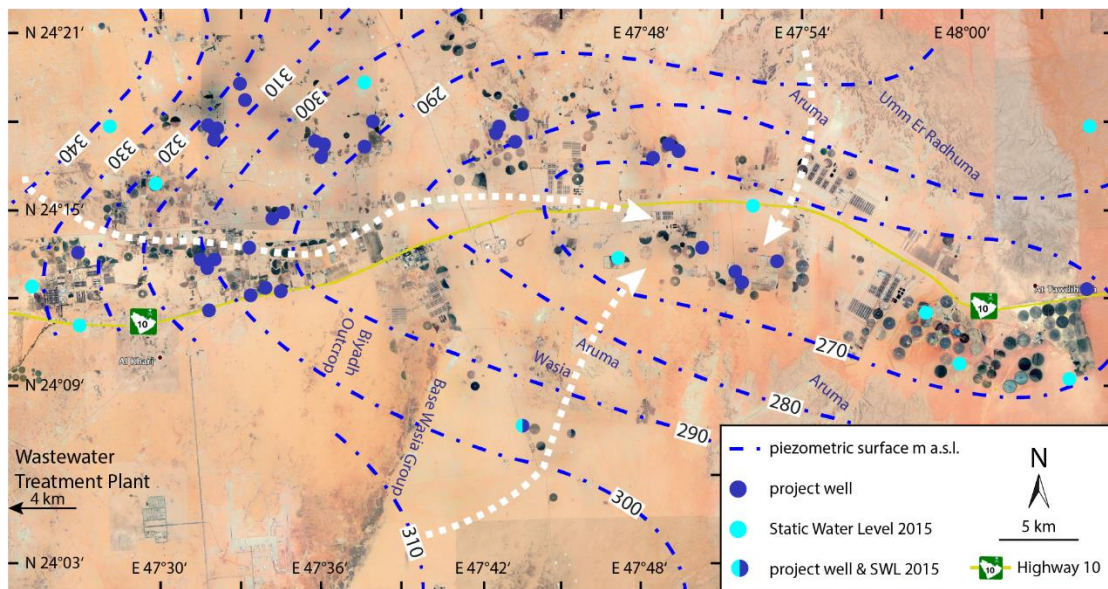


Figure 4. Google Earth map of the study area with sampled wells (dark blue dots) and piezometric heads as of 2015 (updated and modified from Reference [16]). Light blue dots indicate sites of static water level with performed water level measurements. Light blue/dark blue dots represent sampling and piezometric well sites. White, dashed lines are groundwater flow directions. Also shown are some major outcrop areas with dark grey to green colored radial-shaped irrigation areas (center pivots) and the position of the wastewater treatment plant south of Al Kharj.

The Biyadh aquifer is characterized by transmissivity values between $1.26 \times 10^{-3} \text{ m}^2/\text{s}$ to $9.7 \times 10^{-2} \text{ m}^2/\text{s}$ and a storage coefficient between 2.0×10^{-4} and 9.0×10^{-4} [26–28]. Porosity is

very heterogeneous with values ranging from 1.1% to 40% with an average value between 23% and 31%. Similarly, the permeability varies from 0.2 to 27,000 mD with average values between 1700 and 4500 mD [26–29].

The transmissivity of the overlying Wasia aquifer ranges from 1.5×10^{-2} m²/s to 9.7×10^{-2} m²/s and a storage coefficient between 2.3×10^{-7} and 9.0×10^{-4} [26–28] (Table 1). The Wasia aquifer consists of fossil water that has been recharged during cooler climatic conditions [16]. As ¹⁴C dating of the underlying Triassic Jilh aquifer in northwestern Saudi Arabia resulted in a residence time between 25,000 and 35,000 years BP in the Late Pleistocene [30], and of the Paleozoic and Cretaceous aquifer systems in southwestern Saudi Arabia between 2400 and 35,000 years BP [31]. Hence, the Cretaceous Wasia aquifer in the study area was most likely recharged under similar climatic conditions during the Last Glacial Maximum (LGM). The study area lies within a large wadi system with natural springs, which are mostly dried out at present [13]. Porosity and permeability are within a similar range as the Biyadh aquifer [26–29].

Table 1. Hydraulic properties of the Biyadh and Wasia aquifers (modified from [26]).

Biyadh			
Hydraulic Property	Source	Value Range	Average Value
Transmissivity, T	[26]	1.7×10^{-3} – 9.0×10^{-2} m ² /s	3.3×10^{-2} m ² /s
	[27]	1.26×10^{-3} – 7.0×10^{-2} m ² /s	3.6×10^{-2} m ² /s
	[28]	1.5×10^{-2} – 9.7×10^{-2} m ² /s	n/a
Hydraulic conductivity, K	[26]	2.5×10^{-4} – 4.5×10^{-4} m/s	3.0×10^{-4} m/s
	[27]	3.3×10^{-5} – 3.0×10^{-4} m/s	19×10^{-4} m/s
	[26]	2.3×10^{-4} – 9.0×10^{-4}	4.9×10^{-4}
Storage coefficient, S	[27]	n/a	3.2×10^{-2}
	[28]	n/a	2.0×10^{-4}
	[26]	-	5–15% (estimated)
Porosity, Φ	[25]	1.1–36%	23.3%
	[26]	19–40%	31%
	[29]	7–37%	30%
Permeability, k	[25]	0.2–12,678 mD	1698 mD
	[26]	240–11,100 mD	2500 mD
	[29]	2000–27,000 mD	4500 mD
Wasia			
Transmissivity, T	[26]	1.7×10^{-3} – 9.0×10^{-2} m ² /s	3.3×10^{-2} m ² /s
	[27]	n/a	3.2×10^{-2} m ² /s
	[28]	1.5×10^{-2} – 9.7×10^{-2} m ² /s	n/a
Hydraulic conductivity, K	[26]	2.5×10^{-4} – 4.5×10^{-4} m/s	3.0×10^{-4} m/s
	[27]	1.5×10^{-4} – 4.9×10^{-4} m/s	3.2×10^{-4} m/s
	[26]	2.3×10^{-4} – 9.0×10^{-4}	4.9×10^{-4}
Storage coefficient, S	[27]	n/a	2.3×10^{-7}
	[28]	n/a	2.0×10^{-4}
	[26]	-	5–15% (estimated)
Porosity, Φ	[25]	3.3–41.3%	29.46%
	[26]	19–40%	31%
	[29]	7–37%	30%
Permeability, k	[25]	0.7–15,388 mD	2994 mD
	[26]	240–11,100 mD	2500 mD
	[29]	2000–27,000 mD	4500 mD

3. Methodology

The groundwater samples were collected from thirty-four (34) wells tapping the Wasia aquifer in the Al Kharj area from May 2018 to January 2019. Four samples from each well were stored in polyethylene (PE) bottles for anion and cation concentrations and trace element analysis. A total of 19 and 20 samples were analyzed for nitrate isotopes and tritium, respectively. The sampled

wells are mainly used for irrigation and cattle watering. The PE bottles were pre-washed three times with deionized water to avoid sample contamination. The wells were purged for almost one hour before sampling to recover representative water samples. The piezometric water level, pH, EC, and temperature were measured in situ using multi-parameter meters (Hanna HI 9828). Water samples were filtered (0.45 μm) to remove suspended solids and to limit the microbial activity. They were stored in a cooling box below 4 °C to preserve them for subsequent analysis of ions, nitrate isotopes, and tritium. Then, HNO_3 was added to samples for the preservation of trace metals.

Hydrochemical analyses of major, minor, and trace elements were conducted in the Environmental and Hydrology Laboratory at the King Fahd University of Petroleum and Minerals (KFUPM), Dhahran, Saudi Arabia. Anion and cation concentrations in the mg/L range were measured using the Ion Chromatograph Dionex ICS-6000 (IC) using the EPA 9056A standard method. Bicarbonate was measured using the titration method. The inductively coupled plasma mass spectrometry (iCAP RQ ICP-MS) technique with the EPA 6020A method was applied to measure trace elements within $\mu\text{g/L}$ range. Isotope analyses were conducted at the Environmental Isotope Laboratory, University of Waterloo, Ontario, Canada (^3H , $^{15}\text{N}\text{-NO}_3$, and $^{18}\text{O}\text{-NO}_3$). For nitrate isotopes, NO_3^- was converted to NO_2^- using a cadmium catalyst, then chemically converted to N_2O and subsequently analyzed on a Trace Gas-GVI IsoPrime-IRMS (TG-IRMS) [32]. Tritium measurements were conducted using a liquid scintillation counting (LSC) technique. To increase the precision and lowering the detection limit, samples were counted after being enriched 15 times by electrolysis. This process resulted in a detection limit of 0.8 ± 0.8 tritium units (TUs).

Golden Software Surfer 14, Microsoft Excel 2013, Adobe Illustrator CC 2018, and OriginPro 2016 were used as principal software tools for processing and plotting the data and for map drawing.

4. Results

The hydrochemical composition and isotope ratios ($^{15}\text{N}\text{-NO}_3$, $^{18}\text{O}\text{-NO}_3$, and ^3H) of groundwater samples from the Wasia aquifer in the study area are summarized in Table 2. The average pH value was 7.6 and ranges from 6.8 to 8.0. The average TDS value of these samples was 3030 mg/L with a minimum and maximum of 1100 mg/L and 7710 mg/L, respectively. Wells with the highest TDS (4940–7710 mg/L) and nitrate concentrations (175–395 mg/L) were encountered in the most northern (WA08) and eastern parts (WB01, WB02, WB03, WB19) of the study area (Figure 5). Generally, Wasia groundwater from the Al Kharj area was reported to be of the Ca–Mg– SO_4 –Cl type [13,14]. Based on the relative proportion between major elements, the studied borehole samples are classified into three groups as shown in the Piper diagram of Figure 6. Group 1 samples (WB02, WB03, WB05, WB06, WB07, WB13, WB14, WB17, WB18, WB19) were a Ca– SO_4 –Cl water type with a broad salinity range from 1580 to 7710 mg/L. Most of the water samples belonged to the second group (WB01, WB04, WB08, WB09, WB10, WB11, WB12, WB15, WB16, WB20, WA03, WA04, WA06, WA07, WA08, WA14) of the Ca– SO_4 type with a similar wide salinity range from 1240 to 6260 mg/L. The third geochemical group (WA01, WA02, WA05, WA09, WA10, WA11, WA12, WA15) was less saline than the other two groups (1100–2400 mg/L) and displayed a Ca–Na– SO_4 –Cl water-type composition. Ca^{2+} represents the dominant cation (119–232 mg/L), followed by Na^+ (115–254 mg/L), Mg^{2+} (36.7–70.6 mg/L), and K^+ (4.35–11.5 mg/L). SO_4^{2-} (234–500 mg/L), Cl^- (136–348 mg/L), and HCO_3^- (153–193 mg/L) are the dominant anions for Group 3. The Ca–Na– SO_4 –Cl (Group 3) and Ca– SO_4 –Cl (Group 1) water samples are located along a W–E trending trench in the northern and central zone of the study area (Figure 5). The Ca– SO_4 –type groundwater (Group 2) is mainly encountered in the peripheral zone of the study area.

Table 2. Hydrochemical parameters, stable isotope ratios of nitrates (15N–NO3 and 18O–NO3), and tritium measurements for selected groundwater samples from the Wasia aquifer in the study area.

Well	pH	T	EC	TDS	TH	Na ⁺	K ⁺	Mg ²⁺	Ca ²⁺	HCO ₃ ⁻	F ⁻	Cl ⁻	NO ₂ ⁻	Br ⁻	NO ₃ ⁻	SO ₄ ²⁻	PO ₄ ³⁻	Li	B	Co	Mn	V	Zn	Fe	As	Ni	Cu	Mo	³ H	δ ¹⁵ N	δ ¹⁸ O	Water Type	
Units	°C	µS/cm	mg/L	mg/L	mg/L	mg/L	mg/L	mg/L	mg/L	mg/L	mg/L	mg/L	mg/L	mg/L	mg/L	mg/L	mg/L	mg/L	µg/L	µg/L	µg/L	± 0.8 T.U.	AIR ± 0.5‰	VSMOW ± 1‰									
WB01	7.3	31.9	6809	5860	1850	433	4.19	159	479	188	1.8	1170	ND	5.5	358	1330	ND	0.9	1150	0.81	3.05	3.24	5.52	3040	0.23	0.51	1.65	7.39	<0.8	5.9	25.8	Ca–SO ₄	
WB02	7.5	32.5	8007	7330	2740	359	4.43	212	747	77.0	1.7	1690	ND	5.9	359	974	ND	ND	449	1.10	4.24	3.87	3.32	4120	0.27	ND	1.72	4.05	<0.8	7.1	24.2	Ca–SO ₄ –Cl	
WB03	7.6	30.5	8673	7710	2890	462	6.97	244	756	89.0	1.8	1840	ND	6.0	395	1190	ND	ND	783	1.00	8.83	2.60	ND	4050	0.21	0.44	2.74	3.71	0.98	5.8	24.6	Ca–SO ₄ –Cl	
WB04	7.6	36.9	2317	1990	686	123	6.36	57.3	180	161	1.2	362	ND	2.6	3.26	405	ND	0.5	328	0.41	88.2	0.15	1.96	1140	ND	0.92	11.15	2.96	<0.8	-	-	Ca–SO ₄	
WB05	7.6	28.4	3684	3370	1540	158	3.30	121	419	147	1.4	375	ND	2.3	25.3	1290	ND	0.5	465	0.54	4.33	2.30	ND	1870	0.09	ND	0.35	3.48	<0.8	10.7	11.2	Ca–SO ₄ –Cl	
WB06	7.8	27.6	4246	3930	1670	207	5.69	138	441	118	1.6	449	ND	2.4	62.0	1440	ND	0.5	469	0.55	8.29	0.35	48.8	1990	ND	ND	2.75	6.78	<0.8	6.6	9.5	Ca–SO ₄ –Cl	
WB07	7.9	31.9	1811	1580	734	67.0	1.98	60.1	195	150	1.5	164	ND	ND	4.97	558	ND	0.5	273	2.17	2.57	1.26	ND	702	ND	1.43	0.82	4.06	<0.8	8.0	16.7	Ca–SO ₄ –Cl	
WB08	7.9	30.3	7585	6260	2160	552	10.9	177	576	187	1.8	1320	ND	5.5	175	1630	ND	0.9	1430	1.34	22.2	3.04	ND	2560	0.04	1.18	1.47	5.05	0.82	7.6	21.9	Ca–SO ₄ –Cl	
WB09	7.7	30.9	3944	3320	1200	229	4.61	105	307	154	1.2	612	ND	2.7	111	779	ND	0.0	555	0.32	0.00	1.79	0.00	1110	0.04	0.00	0.69	3.45	<0.8	6.5	23.4	Ca–SO ₄	
WB10	7.7	31.6	2271	1960	712	116	1.09	61.7	183	148	1.2	310	ND	2.3	47.5	414	ND	0.5	319	0.15	0.00	2.13	0.00	581	0.16	0.00	0.19	2.94	<0.8	7.0	19.9	Ca–SO ₄	
WB11	7.7	32.4	3433	2900	1010	199	3.52	86.7	262	145	1.2	491	ND	2.5	97.4	682	ND	0.5	531	0.28	0.54	1.45	0.00	940	0.10	0.00	0.39	2.77	<0.8	7.0	17.4	Ca–SO ₄ –Cl	
WB12	7.8	34.8	1487	1240	473	67.0	2.39	41.2	122	148	1.2	162	ND	1.2	8.54	278	ND	0.2	195	0.24	8.44	0.72	0.00	459	0.00	0.40	0.13	4.19	<0.8	9.7	13.5	Ca–SO ₄	
WB13	7.9	27.6	4387	3930	1650	224	4.79	138	434	119	1.6	480	ND	2.4	27.4	1450	ND	0.0	535	0.42	2.31	1.93	4.87	1640	0.09	0.71	0.41	5.06	<0.8	10.8	13.5	Ca–SO ₄ –Cl	
WB14	8.0	28.1	3711	3310	1440	167	3.41	112	394	145	1.5	380	ND	2.3	28.9	1220	ND	0.5	383	0.46	6.20	1.35	40.7	1700	0.08	0.85	1.93	5.39	<0.8	9.9	13.0	Ca–SO ₄ –Cl	
WB15	7.7	34.2	3458	2900	1070	184	2.80	84.1	291	140	1.2	516	ND	2.7	76.7	681	ND	0.5	363	0.29	1.04	1.69	0.00	1140	0.15	0.00	0.39	3.21	<0.8	5.5	18.5	Ca–SO ₄	
WB16	7.8	31.9	3327	2850	1030	159	3.55	83.7	273	143	1.2	497	ND	2.8	63.1	591	ND	0.5	278	0.23	ND	0.67	ND	870	ND	0.35	0.11	7.11	<0.8	5.9	20.6	Ca–SO ₄	
WB17	7.9	29.0	2912	2540	1120	122	3.11	87.9	304	142	1.6	282	ND	2.2	36.8	906	ND	0.5	338	0.64	ND	0.72	ND	989	ND	ND	0.37	5.08	<0.8	7.9	13.2	Ca–SO ₄ –Cl	
WB18	7.7	29.7	2595	2250	999	103	1.84	76.6	274	142	1.6	233	ND	2.2	21.5	831	ND	ND	293	0.26	17.7	0.23	ND	960	ND	ND	1.43	4.32	<0.8	8.5	8.7	Ca–SO ₄ –Cl	
WB19	7.9	30.1	5588	4940	1810	289	3.37	148	482	109	1.8	1030	ND	5.0	206	923	ND	ND	516	0.43	1.36	3.64	ND	1630	0.22	ND	0.58	3.87	<0.8	5.7	21.7	Ca–SO ₄ –Cl	
WB20	7.9	30.7	1680	1450	535	76.0	1.38	47.2	137	118	1.3	201	ND	ND	18.4	328	ND	0.4	246	0.09	2.83	3.20	ND	419	0.30	ND	0.50	5.01	<0.8	7.9	17.8	Ca–SO ₄	
WA01	7.5	35.0	1536	1100	449	115	5.47	36.7	119	165	1.0	136	ND	0.96	2.41	237	ND	66.3	334	0.42	1.27	2.25	ND	68.2	0.13	0.09	0.42	7.62	-	-	-	Ca–Na–SO ₄ –Cl	
WA02	7.2	36.0	2504	1990	694	215	5.53	59.9	179	169	0.85	272	ND	1.14	9.54	417	ND	68.5	467	0.60	2.48	2.30	1.7	72.8	0.17	0.38	0.89	4.38	-	-	-	Ca–Na–SO ₄ –Cl	
WA03	6.8	32.5	5255	4920	1690	395	7.40	134	457	168	1.4	780	ND	2.94	25.2	754	ND	71.4	399	1.50	20.9	3.03	ND	110	0.21	0.32	1.98	3.37	-	-	-	Ca–SO ₄	
WA04	7.2	29.5	3746	3180	1400	288	5.30	111	380	169	1.6	304	ND	1.85	6.86	1200	ND	53.8	407	1.68	7.90	0.84	36.3	83.7	0.04	1.01	1.83	5.90	-	-	-	Ca–SO ₄	
WA05	7.3	32.0	2237	1720	642	187	4.35	53.4	169	193	0.87	239	ND	1.14	8.25	349	ND	51.3	325	0.44	0.05	2.73	2.66	33.7	0.20	0.26	0.63	3.97	-	-	-	Ca–Na–SO ₄ –Cl	
WA06	7.4	31.5	2170	1820	747	147	11.3	57.6	204	153	1.13	161	0.2	1.03	94.0	562	8.7	34.6	375	1.88	1.21	1.82	0.91	38.8	0.06	0.66	0.94	6.49	-	-	-	Ca–SO ₄	
WA07	6.9	32.3	2440	2070	904	169	5.59	72.7	242	160	1.07	175	0.1	1.01	1.90	725	7.3	40.9	380	0.88	1.27	0.52	ND	41.4	0.01	0.31	1.09	5.37	-	-	-	Ca–SO ₄	
WA08	6.9	31.4	1310	1860	754	207	6.96	62.1	200	68	1.25	186	0.2	1.05	1.94	625	ND	14.8	161	2.74	1.71	0.37	2.82	87.3	0.02	1.72	0.10	1.13	-	-	-	Ca–SO ₄	
WA09	7.2	32.8	2970	2420	869	254	6.71	70.6	232	167	0.87	348	0.1	1.45	10.3	500	ND	81.6	418	0.73	0.22	2.90	0.00	39.6	0.22	0.31	1.04	5.58	-	-	-	Ca–Na–SO ₄ –Cl	
WA10	7.3	35.5	1970	1500	566	152	6.70	45.4	152	153	0.89	212	0.1	1.31	<1	304	ND	78.2	299	1.02	32.3	0.19	1.45	38.9	0.37	0.23	0.64	18.9	-	-	-	Ca–Na–SO ₄ –Cl	
WA11	7.7	35.8	2360	1780	746	185	11.5	59.9	200	179	0.74	237	0.2	1.32	<1	463	ND	44.3	134	0.19	20.2	0.08	ND	18.3	0.01	0.10	0.26	0.86	-	-	-	Ca–Na–SO ₄ –Cl	
WA12	7.5	36.7	2310	1810	680	207	6.60	59.2	175	164	0.92	256	ND	1.19	7.97	419	ND	68.4	429	0.53	1.18	3.19	ND	20.5	0.24	0.23	0.94	4.67	-	-	-	Ca–Na–SO ₄ –Cl	
WA14	7.4	28.5	4040	3580	1510	329	7.22	118	411	137	1.91	335	ND	2.25	14.7	1260	ND	86.8	693	3.60	5.09	1.41	ND	114	0.05	1.54	2.59	10.4	-	-	-	Ca–SO ₄	
WA15	7.7	31.4	2240	1720	639	201	5.42	53.0	168	164	0.97	244	0.1	1.12	8.16	377	ND	63.2	403	0.52	0.36	4.02	ND	52.9	0.35	0.36	0.98	5.13	-	-	-	Ca–Na–SO ₄ –Cl	

Notes: EC: Electrical Conductivity; TDS: Total Dissolved Solids; TH: Total Hardness; T.U.: Tritium Units; AIR: Atmosphere of Earth; VSMOW: Vienna standard mean ocean water.

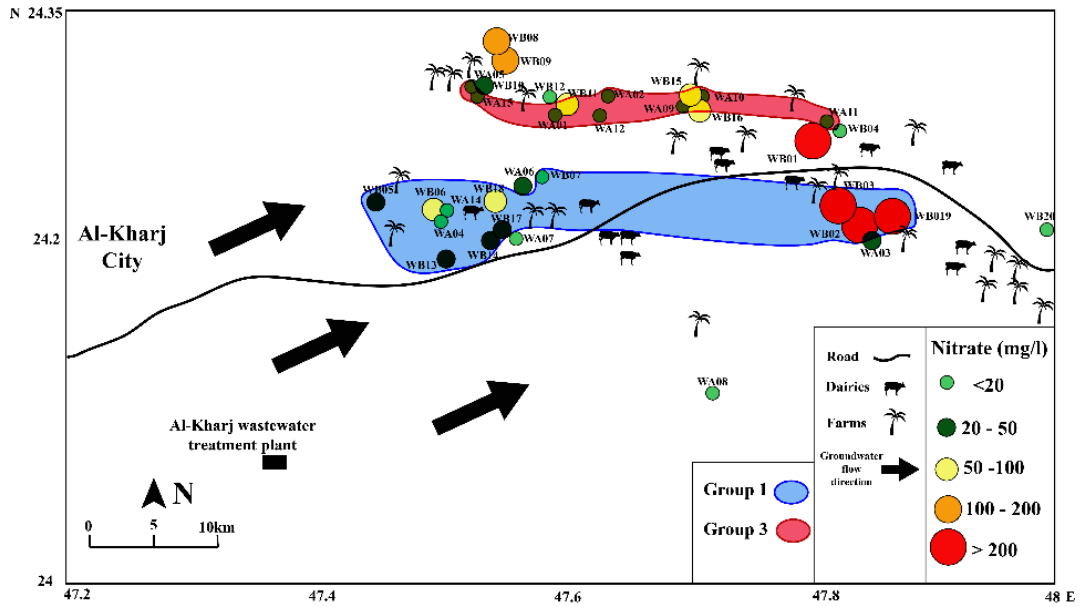


Figure 5. Map of measured nitrate concentrations in the Wasia aquifer and land use in the Al Kharj study area. Also shown is the attribution of water samples to Groups 1 and 3 according to the Piper diagram (Figure 6). All other shown sample sites belong to Group 2.

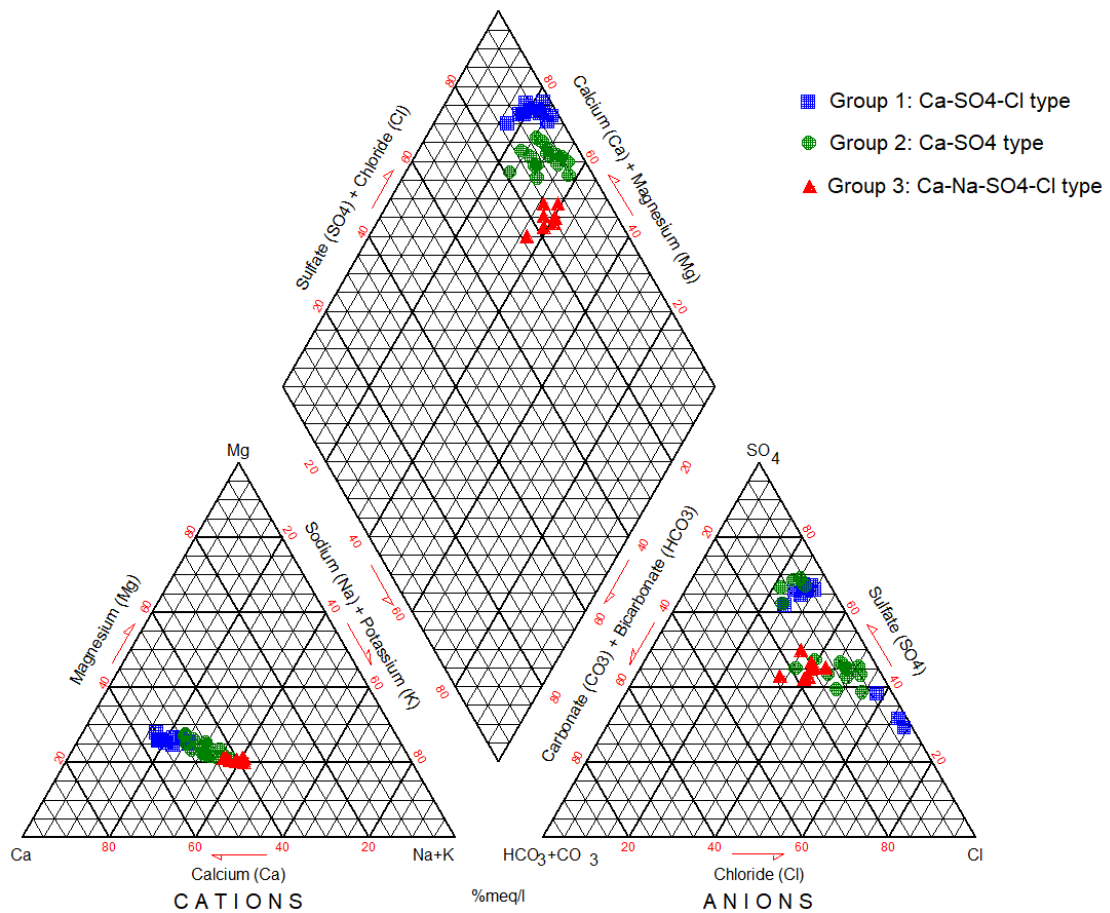


Figure 6. Piper classification diagram with the three hydrochemical groups of groundwater identified from the Wasia aquifer in the Al Kharj area.

The NO_3^- concentrations reached up to 395 mg/L in some wells with an average of 68.2 mg/L. Spatially, wells with high nitrate concentrations (>100 mg/L) are distributed in the eastern (WB01, WB02, WB03, and WB19) and northwestern (WB08 and WB09) parts that are dominated by farms (Figure 4). Eleven out of 34 analyzed Wasia groundwater samples exceeded the WHO drinking water guideline value for nitrate of 50 mg/L [33]. Nitrate concentrations below the WHO guideline are mostly encountered in the peripheral zone of the study area with the highest sample density in the southwest (Figure 5). Li and Fe are the most dominant trace elements in present fluid samples with an average of 445 $\mu\text{g/L}$, 24.5 $\mu\text{g/L}$, and 963 $\mu\text{g/L}$, respectively. Nitrate isotope ratios from the Wasia aquifer ranged from 5.5‰ to 11.3‰ versus AIR (atmosphere of Earth) and from 8.6‰ to 25.8‰ versus VSMOW (Vienna standard mean ocean water) for $\delta^{15}\text{N}-\text{NO}_3$ and $\delta^{18}\text{O}-\text{NO}_3$, respectively.

Two out of 20 analyzed samples in the northwestern (WB08) and eastern area (WB03) showed tritium (^3H) concentrations of 0.82 ± 0.8 TU and 0.98 ± 0.8 TU, respectively, while the remaining samples presented readings below the detection limit of 0.8 TU (Table 2). The analytical results are discussed in the upcoming section.

5. Discussion

5.1. Tritium for Recent Recharge Assessment

Tritium analyses of precipitation samples from 12 rainfall events in Riyadh yielded concentrations between 2.8 and 6.4 tritium units (TU) which are close to the natural background of a few TU [34]. For the present Wasia groundwater samples (except WB03 and WB08), ^3H concentrations below the detection limit of 0.8 TU implied the absence of recent recharge with a residence time beyond the 1950s or 1960s. It is very likely, that the Cretaceous Wasia aquifer was recharged during the Last Glacial Maximum in the Late Pleistocene, as documented for the Triassic Jilh aquifer in northwestern Saudi Arabia [30], for the lower and upper Wajid aquifers, and the combined Wasia–Biyadh–Aruma aquifer in southwestern Saudi Arabia [31]. A second option could be the mixture of a recent surface water source with fossil groundwater. The samples WB03 and WB08 with detectable tritium concentrations (0.98 ± 0.8 TU and 0.82 ± 0.8 TU, respectively, Table 2) were characterized by most elevated salinity (6260–7710 mg/L), nitrate (175–395 mg/L), and boron (780–1430 $\mu\text{g/L}$) concentrations. This combination suggests the local influx of evaporated irrigation water with remnants of dissolved fertilizer into the Wasia groundwater system in the vicinity of these two wells. It can be concluded that samples with tritium concentrations below 0.8 TU are composed of fossil water that has likely been recharged during the Late Pleistocene, while the samples “WB03” and “WB08” could present some additional atmospheric influx from infiltrated irrigation water.

As the applied LSC technique is limited to a detection limit to 0.8 TU, more advanced techniques like helium (^3He) ingrowth may be needed to reach higher precision. The helium ingrowth method depends on measuring helium concentrations that decay from tritium after storing the groundwater sample for several months and then normalized to a reference date to reconstruct the tritium content. This method can reach a detection limit of up to 0.005 TU [3].

5.2. Possible Sources of Nitrate

Ammonium, nitrate fertilizers, manures or animal waste as potential anthropogenic sources and nitrogen input by precipitation/atmospheric deposition or from interaction with rock or soil as natural sources for the accumulation of nitrate in the Wasia aquifer in the study area (Figures 7 and 8) are discussed in this chapter.

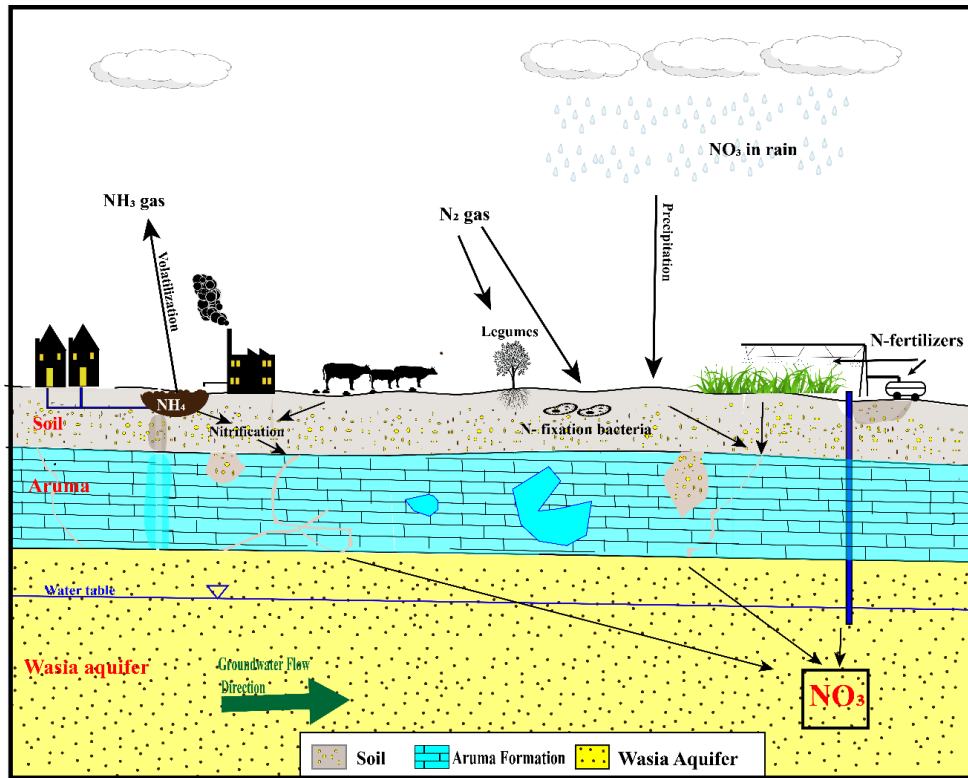


Figure 7. Schematic diagram of potential natural and anthropogenic sources for nitrate in the Al Kharij area.

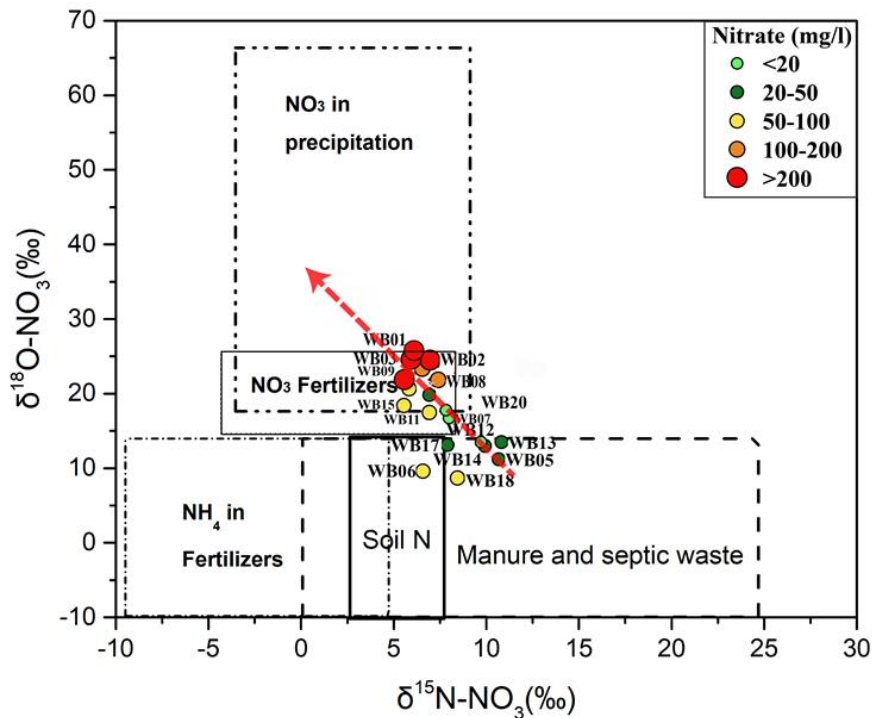


Figure 8. Relationship between $\delta^{15}N_{NO_3}$ and $\delta^{18}O_{NO_3}$ isotopes of analyzed groundwater samples from the study area. General ranges for the isotopic compositions of different types of common nitrate sources were adapted from Reference [35]. The increasing nitrification of Wasia groundwater by the influx of fertilizer is shown by the red arrow.

5.2.1. Fertilizers

As the study area is dominated by agricultural activities, several fertilizers are added to the soil. It is critical to differentiate between synthetic nitrate fertilizers by industrial fixation of atmospheric nitrogen and nitrate resulting from ammonium fertilizers. The former generally have a $\delta^{15}\text{N}$ range of -5‰ to $+8\text{‰}$ and higher $\delta^{18}\text{O}$ of $+17\text{‰}$ to $+25\text{‰}$, as it is derived from atmospheric oxygen. The influx of ammonium fertilizer causes a wider range of $\delta^{15}\text{N}_{\text{NO}_3}$ due to the various sources (-10‰ to $+5\text{‰}$) and more depleted ratios for $\delta^{18}\text{O}_{\text{NO}_3}$ (-15‰ to $+15\text{‰}$) [6].

In the present case study, the combination of most depleted $\delta^{15}\text{N}_{\text{NO}_3}$ and most elevated $\delta^{18}\text{O}_{\text{NO}_3}$ ratios for recovered groundwater samples in the most northern (WB08, WB09) and eastern (WB01, WB02, WB03, WB19) section of the study area (Figures 8 and 9) suggest that synthetic fertilizers represent the main local source for nitrate. Where ammonium fertilizers generally have a lower range of $\delta^{18}\text{O}_{\text{NO}_3}$, 63% of the studied samples fall within the area of the isotopic composition of synthetic nitrate fertilizers ($+5.5\text{‰}$ to $+8.0\text{‰}$ and $+16.7\text{‰}$ to $+25.8\text{‰}$ for $\delta^{15}\text{N}$ and $\delta^{18}\text{O}$, respectively). In contrast, the combination of lower saline conditions (TDS = 1400–2000 mg/L), elevated $\delta^{15}\text{N}_{\text{NO}_3}$ and depleted $\delta^{18}\text{O}_{\text{NO}_3}$ ratios in the western part of the study area (western flank of Water Group 1 and 3 from Section 4 and in Figure 4) indicate the presence of pristine Wasia groundwater with minimum alteration by anthropogenic factors. The negative isotope trend in Figure 8 illustrates the increasing nitrification of the Wasia aquifer by the influx of fertilized irrigation water.

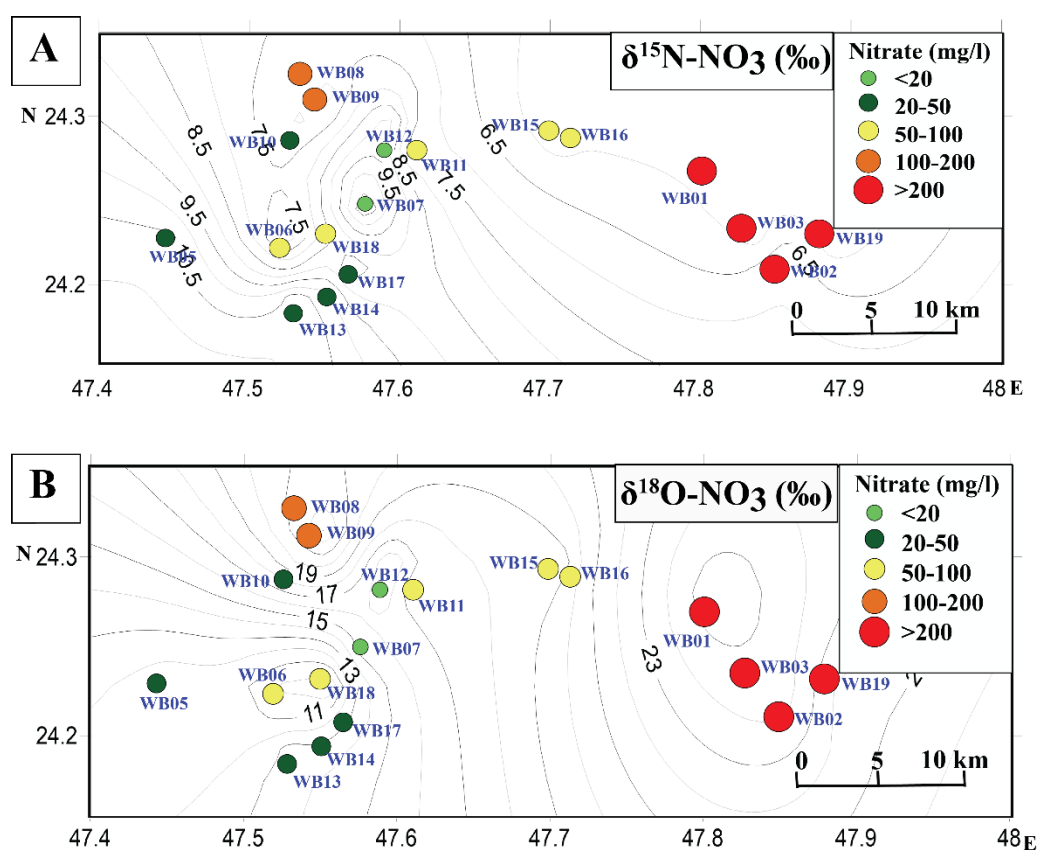


Figure 9. Spatial distribution of (A) $\delta^{15}\text{N}$ and (B) $\delta^{18}\text{O}$ of nitrate from Wasia groundwater wells in the Al Kharj area.

Boron occurs naturally in groundwater, but high levels of boron may indicate anthropogenic sources such as landfill leachate, drainage from coal mines and mining related wastes, and sewage effluent due to the fact of its presence in detergents. Boron can be concentrated in agricultural as it is a minor constituent in fertilizers and pesticides [36,37]. Although none of the water samples

exceeded the recent WHO recommendation of 2400 $\mu\text{g/L}$ for boron in drinking water [38], the boron concentrations between 520 and 1430 $\mu\text{g/L}$ for seven samples (WB01, WB03, WB08, WB09, WB11, WB13, and WB19) were above the recommended WHO norm from 2017 of 500 $\mu\text{g/L}$ [38]. These wells are distributed in the northwestern and eastern parts of the study area and are positively linked to wells with elevated nitrate concentrations. The presence of boron in these wells suggests the influx of fertilizers in these parts of the study area, as previously illustrated by nitrogen and oxygen isotopes. Two of the potential fertilizer-affected samples (WB03, WB08) also show relatively elevated tritium concentrations, which suggest the infiltration of recent water into the Wasia aquifer.

5.2.2. Atmospheric Deposition

Rainwater analysis in the study region showed average concentrations of 4.26 mg/L for NO_3^- and 17.4 mg/L for Cl^- [39]. A precipitation rate of 75 mm per year [16] would result in an annual deposition of around 3.2 kg/ha of NO_3^- which will possibly be taken up by vegetation, soil bacteria, or might percolate to the water table. As part of a mass balance, this calculated amount of nitrate alone does not account for the entire nitrate budget.

With an annual average recharge of 5 to 10 mm [16] and elevated evaporation rates that reach 2000 mm/year [16,22], evaporation is anticipated to play a major role in nitrate accumulation in the Wasia aquifer. Considering exclusively the effect by evaporation, mentioned recharge rates, and an average annual rainfall rate of 75 mm in this area [16], an evaporation rate of about 87% to 93% is required to decrease the precipitated rainwater volume to the recharge amount. Considering the Cl^- concentration as a measure for the rate of evaporation, the analyzed Cl^- concentrations between 136 and 1840 mg/L in this groundwater could result from an evaporation rate of 87% to 99% of rainwater with 17.4 mg/L of Cl^- . A concentration of 33 to 426 mg/L of nitrate might result from this simulated scenario of evaporation, which agrees with measured nitrate concentrations in the studied samples. The detected linear relationship between Cl^- and NO_3^- concentrations, especially for most saline samples suggests the influence of evaporation as an essential contributor for Cl^- and NO_3^- enrichment in the studied Ca Wasia aquifer (Figure 10a). The excellent correlation between Cl^- as a conservative element and Ca^{2+} as a reactive element confirms the lack of secondary water–rock alteration processes (Figure 10b). According to stable isotope ratios of nitrate ($^{15}\text{N}\text{-NO}_3$ and $^{18}\text{O}\text{-NO}_3$), 58% of these nitrate concentrations (11 out of 19 samples) are related to atmospheric deposition (Table 2 and Figure 8). Atmospheric deposition is apparently a major contributor to the elevated nitrate concentrations in the Wasia aquifer, although reduced amounts by vegetation, fixation bacteria, and other factors cannot be predicted.

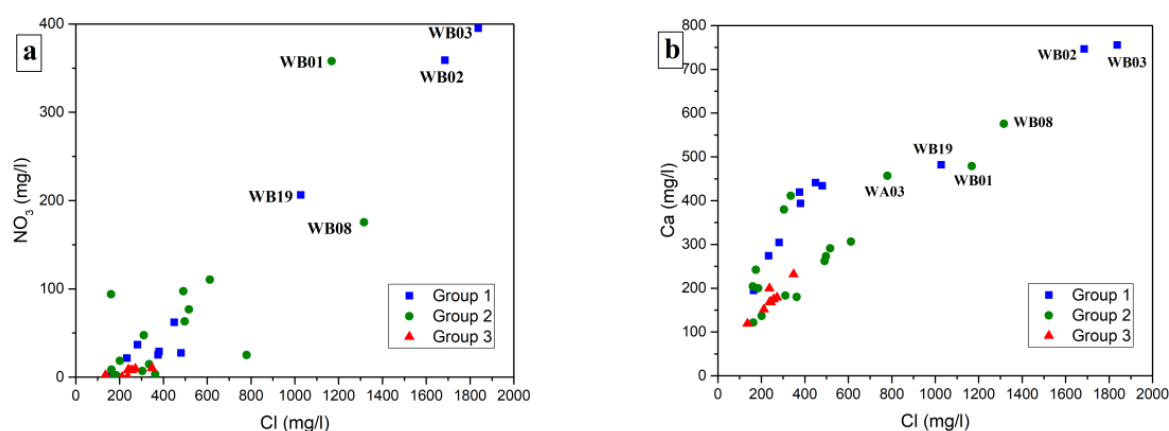


Figure 10. Cl^- versus NO_3^- (a) and Cl^- versus Ca^{2+} (b) concentrations of 34 groundwater samples from the Al Kharj area.

5.2.3. Nitrogen from Animal and Human Waste (Manures)

The dominant nitrogen compound in animal and human wastes is urea. The enzyme urease hydrolyzes the urea to ammonium and then to nitrate in the vadose zone, where it can percolate down to the water table [3]. The hydrolysis of urea results in a momentary increase in pH that helps the transformation to NH_3 gas, which is released to the atmosphere.

The studied water samples from the Wasia aquifer have no or undetectable concentrations of ammonia. Depending on the availability of oxygen, NH_4^+ may be oxidized and detected only as NO_3^- . Therefore, N input from animal or human waste may not be detected as ammonium. The presence of iron in the groundwater also helps nitrifying bacteria in ammonia oxidization to nitrite and then to nitrate [40,41]. Besides elevated nitrate concentrations, groundwater affected by manures usually has high Cl^- and K^+ amounts [3]. While K^+ is basically low (<11.5 mg/L) in the studied Wasia aquifer, a strong correlation between Cl^- and NO_3^- was found in the samples (Figure 10). The effect of manure on the hydrochemical composition of the Wasia aquifer seems to be negligible or minor, as NH_4 , PO_4 , and NO_2 are absent in those samples.

5.2.4. Nitrogen from Rocks

Elevated nitrogen in rocks has been measured in igneous, metamorphic, and especially in sedimentary deposits and metasediments [10]. Nitrogen is easily weathered under surface conditions, and it can be discharged as a solution in the saturated zone due to the high solubility of nitrate salts [3]. The Wasia Group, which represents the main aquifer in the Al Kharj area, generally consists of sandstone, conglomerate, and shale layers [23,25,42]. As there is no mention of nitrate salts present in the Wasia Group and the underlying and overlying rocks, it is unlikely that such salts are source for nitrate in the studied groundwater samples.

5.2.5. Soil Nitrogen

Nitrogen may exist naturally in the soil, as some symbiotic soil bacteria fix atmospheric nitrogen. Nitrogen also occurs in plants like the legume family [43]. These processes take part in the nitrogen cycle. This accumulation of nitrate in the unsaturated zone can form a large nitrate pool which may infiltrate to the saturation zone during recharge periods. Although the isotopic composition of one of the studied samples (WB06) lies within the soil nitrogen area (Figure 8), it is unlikely that soil nitrogen has contributed to the nitrogen content in the studied samples. This sample may have been affected by manure and wastewater nitrogen.

5.3. Estimating N Fluxes

To evaluate whether the rates of nitrate percolation to the aquifer and recharge amount are sufficient to explain the nitrate concentration in the studied samples, the estimated nitrate fluxes were compared to the calculated aquifer exchange time. Considering an average thickness of 100 m, 30% of effective porosity, and a recharge rate of 5 to 10 mm/year for the aquifer in the study area [16], a direct water budget calculation resulted in a required 3000 to 6000 years for the complete exchange of water assuming steady-state conditions. The average nitrate concentration measured in the groundwater of this study (68.2 mg/L) would give around 20,000 kg/ha of overall nitrate for a 100 m aquifer thickness. Based on the time required to exchange the geochemical composition of the aquifer, an average 3.34 to 6.67 kg/(ha) per year of nitrate flux would be required to match the overall nitrate in the aquifer. This calculated amount of nitrate flux cannot be explained by one single source. Therefore, a combination of synthetic fertilizers and atmospheric deposition is most likely to be responsible for the detected nitrate concentrations. This interpretation coincides with a regional groundwater survey in Saudi Arabia, where 213 out of 1060 wells were encountered to exceed the maximum limit of 50 mg/L for nitrate in drinking water [44]. Most affected wells were reported in areas, listed in descending order, with agricultural–residential, agricultural, housing–desert, housing, desert, and industrial land use.

5.4. Wasia Aquifer: Mixing Model and Nitrate Provenance

Wells with the lowest salinity concentrations between 1100 and 2000 mg/L in the Al Kharj area are generally coupled to low nitrate concentration with values below 20 mg/L (Figure 10a). Therefore, low saline groundwater samples from Ca–SO₄–Cl (Group 1) and Ca–SO₄ (Group 2) water types, plus all Ca–Na–SO₄–Cl type samples (Group 3) are considered to represent pristine fluids from the Wasia aquifer without anthropogenic input or influx from the surface (Figure 10a,b). The salinity range (1100–2000 mg/L) for Wasia groundwater in the Al Kharj area is even lower than the reported TDS concentration of 2500 mg/L for the Wasia–Biyadh aquifer in the region west of Khurais [45]. In contrast, elevated nitrate, chloride, TDS, and ¹⁸O–NO₃ values (up to 395 mg/L) and depleted ¹⁵N–NO₃ ratios of water samples from two local spots in the northern (WB08, WB09) and eastern (WB01, WB02, WB03, WB19) part of the study area imply the mixing of pristine Wasia groundwater with surface water influx. The positive correlation between Cl, Ca, and NO₃ suggests the presence of two sources (Figure 11). Arid climatic conditions triggered the extreme evaporation of irrigation water on crop areas, with the subsequent infiltration of fertilizer- and salt-enriched irrigation water into the Wasia aquifer system.

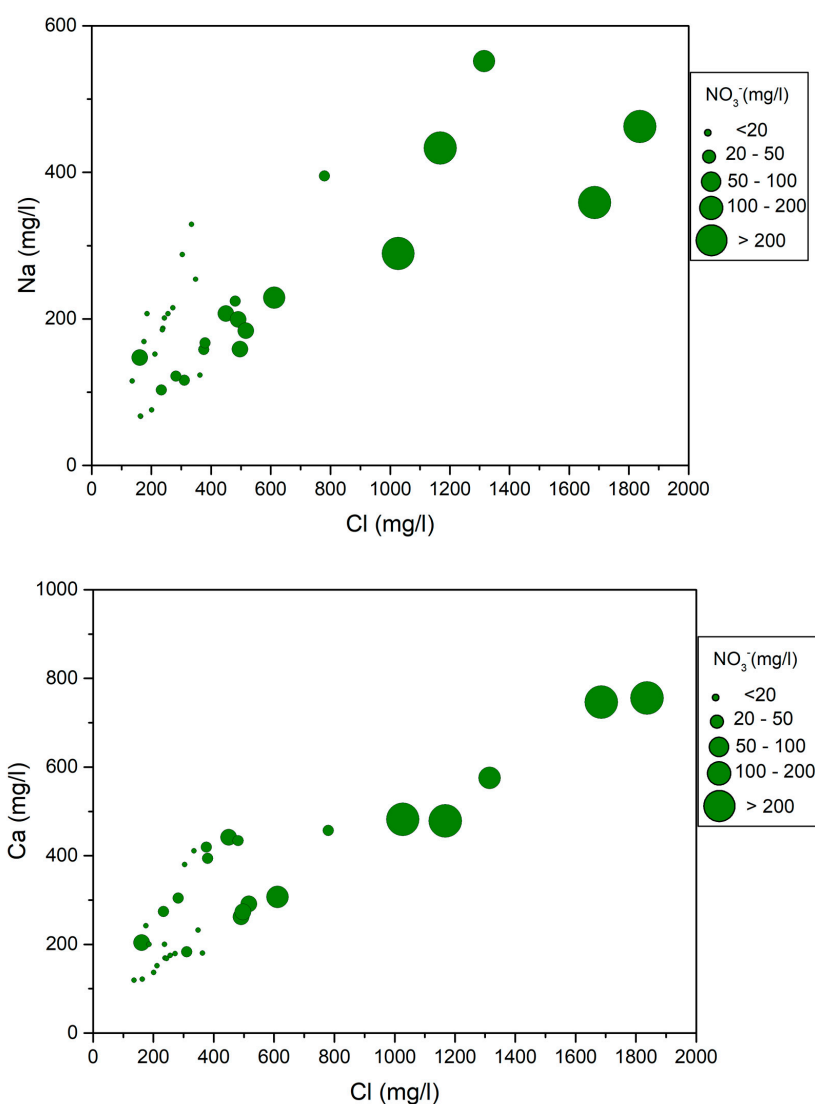


Figure 11. Positive compositional correlation between NO₃²⁻ and Cl⁻, Ca²⁺, and Na⁻ in Wasia groundwater in the Al Kharj area.

The heterogeneous composition of 20 Wasia groundwater samples from 2015 with a minimum and maximum concentration of 1433 to 5619 mg/L for TDS and 24.5 to 378 mg/L for NO_3^- [14] is the same range as that of the present sampling. The geochemical similarity reflects the continuous impact of agricultural activities on the shallow groundwater system in the Al Kharj region

The comparison of specific land use zones in the study area with anomalies in nitrate concentration in groundwater was performed to validate the potential local influx of fertilizer-enriched irrigation water in crop areas. In theory, groundwater in crop areas should be a major target for fertilizer influx. The satellite map in Figure 12 illustrates areas with dominant housing, dairy, poultry, and agricultural farms as dominant land use types. The wells WB02, WB03, and WB09 with the highest nitrate concentrations (206–395 mg/L) are located within an agricultural zone in the eastern part of the study area, where dark-grey to greenish circles reflect the active use of radial irrigation sprinklers. In contrast, water samples from the wells WB08 and WB09 in the northern zone have also elevated nitrate concentrations (111–175 mg/L), but no current residential or agriculture land use can be identified in their neighborhood on satellite images. Generally, none of the sampled supply wells was located within housing, dairy or poultry areas, but some specific wells show slightly elevated nitrate concentrations close to active rural, industrial or agricultural zones. Samples from the wells WB13, WB14, and WB17 are located east of a local housing area (Figure 12). The eastward-directed groundwater flow could explain the presence of slightly elevated nitrate concentrations (27.4–36.8 mg/L) for the mentioned wells. Most of the groundwater wells are located outside the populated and farmed zones and are generally not affected by anthropogenic nitrate, as reflected by concentrations between <1 mg/L and 15 mg/L.

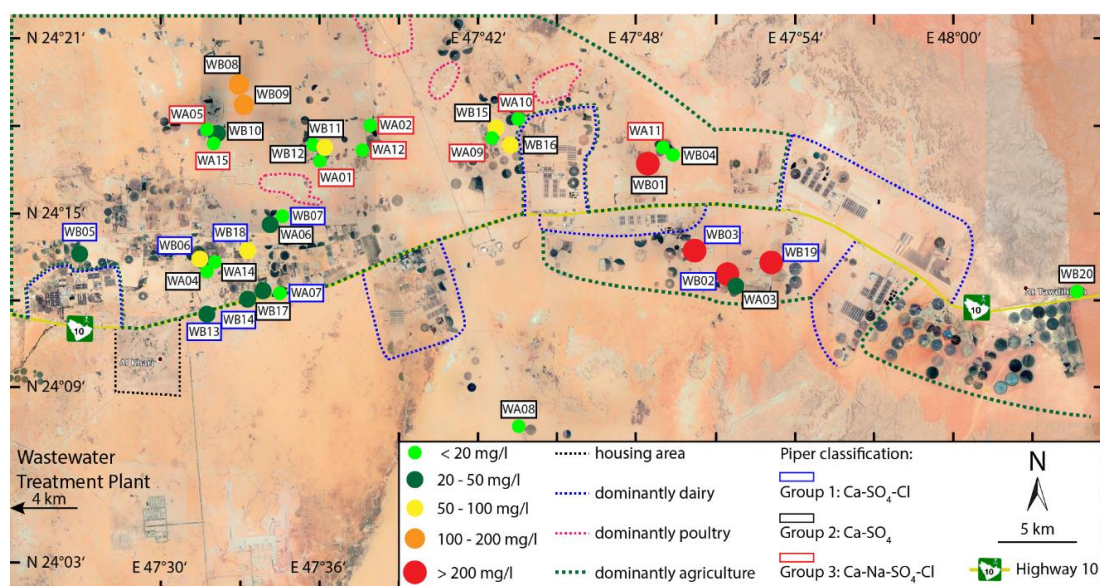


Figure 12. Google Earth map of measured nitrate concentrations of Wasia–Biyadh groundwater in project wells, well numbers, and areas of dominant land use in the study area.

Well WB20 at the most eastern edge of an extensive irrigation field in the most eastern part of the study area is not affected by the proximity distance to an extensive irrigation area, as reflected by minor nitrate concentration of 18.4 mg/L. Potential reasons could be the diversified application of fertilizers for different agricultural products. In the present case, large radial irrigation areas for the watering of alfalfa are probably less demanding for the use of fertilizer, therefore infiltrating irrigation water is less contaminated with nitrate.

6. Conclusions

Source-related signatures of $^{15}\text{N}-\text{NO}_3^-$ and $^{18}\text{O}-\text{NO}_3^-$ were measured in groundwater samples from the Cretaceous Wasia aquifer in central Saudi Arabia. Two local spots in the eastern and northern

parts of the study area are characterized by atmospheric and fertilizers-derived nitrate as inferred from $^{15}\text{N}\text{-NO}_3$ and $^{18}\text{O}\text{-NO}_3$ signatures, and distinguished by adjacent areas by elevated salinity, B, NO_3 , and $\delta^{18}\text{O}_{\text{NO}_3}$ values. The high salinity of 4940 to 7330 mg/L could be an influx of evaporated irrigation water, connate water or a mixture of both sources.

The lowest saline groundwater samples (TDS = 1400–2000 mg/L) from the peripheral and southwestern zone of the study area were representative for pristine groundwater from the Wasia aquifer with nitrate concentrations below 20 mg/L, low $^{18}\text{O}\text{-NO}_3$ ratios (8.7–20.6‰), but had the highest $^{15}\text{N}\text{-NO}_3$ ratios (up to 10.8‰). There was no evidence for the influx of animal or human waste from adjacent dairy farms, poultry farms and housing settlements. Higher saline samples (4940 to 7330 mg/L) from local wells in the eastern and northern part of the Al Kharj region were enriched in NO_3 (up to 395 mg/L), and their negative trend with enrichment in $^{18}\text{O}\text{-NO}_3$ and depletion in $^{15}\text{N}\text{-NO}_3$ reflects the nitrification of Wasia groundwater by fertilizer.

The low tritium (^3H) concentration of the Wasia groundwater, however, indicates the absence of recent recharge or the mixture of recent influx with fossil waters. This is corroborated by the calculated percolation time of between 3000 years and 6000 years needed to effectively exchange the groundwater on a local scale. Tritium concentrations below the detection limit of 0.8 TU could be correlated to a late Pleistocene recharge event of the Wasia aquifer as observed for the underlying Paleozoic and Triassic Jilh aquifers using the radiocarbon dating method [30,31]. The samples “WB03” and “WB08” with the highest tritium and nitrate concentrations may indicate the influx of recent surface water. It can be concluded that natural sources, such as atmospheric deposition as well as anthropogenic sources of N-fertilizer, contribute to the nitrogen budget and to spatial heterogeneities of the Wasia aquifer.

Author Contributions: A.K. wrote, conducted, and analyzed experimental data of this research. A.A.-S. was responsible for designing and analyzing the work. P.B. provided constructive comments, reviews, and edits for this manuscript. M.M. and B.T. contributed to the discussion of the results and to the analysis. M.K. provided constructive comments and edits. All authors have read and agreed to the published version of the manuscript.

Funding: This research was funded by the College of Petroleum Engineering and Geosciences (CPG), King Fahd University of Petroleum and Minerals (KFUPM) under the startup fund number (SF18061).

Acknowledgments: The authors would like to acknowledge the College of Petroleum Engineering and Geosciences (CPG), King Fahd University of Petroleum and Minerals (KFUPM), for the funding and support, and providing facilities for the present study. We greatly appreciate the support of Abdullatif Al-Shuhail. We thank the Exploration Geospatial and Data Management Solutions Division at Saudi Aramco for adjusting the boundaries and coordinates of provided maps.

Conflicts of Interest: The authors declare no conflict of interest.

References

1. Widory, D.; Kloppmann, W.; Chery, L.; Bonnin, J.; Rochdi, H.; Guinamant, J.L. Nitrate in groundwater: An isotopic multi-tracer approach. *J. Contam. Hydrol.* **2004**, *72*, 165–188. [[CrossRef](#)] [[PubMed](#)]
2. Postma, D.; Boesen, C.; Kristiansen, H.; Larsen, F. Nitrate reduction in an unconfined sandy aquifer: Water chemistry, reduction processes, and geochemical modeling. *Water Resour. Res.* **1991**, *27*, 2027–2045. [[CrossRef](#)]
3. Stadler, S.; Osenbrück, K.; Knöller, K.; Suckow, A.; Sültenfuß, J.; Oster, H.; Himmelsbach, T.; Hötzl, H. Understanding the origin and fate of nitrate in groundwater of semi-arid environments. *J. Arid Environ.* **2008**, *72*, 1830–1842. [[CrossRef](#)]
4. Hem, J.D. *Study and Interpretation the Chemical of Natural of Characteristics Water*, 3rd ed.; USGS: Alexandria, Egypt, 1985; Volume 2254, ISBN 2254.
5. Stadler, S. *Investigation of Natural Processes Leading to Nitrate Enrichment in Aquifers of Semi-Arid Regions*; University of Karlsruhe: Karlsruhe, Germany, 2006.
6. Kendall, C.; Elliott, E.M.; Wankel, S.D. Tracing anthropogenic inputs of nitrogen to ecosystems. In *Stable Isotopes in Ecology and Environmental Science*, 2nd ed.; Michener, R., Lajtha, K., Eds.; Blackwell Publishing Ltd.: Oxfordshire, UK, 2007; Chapter 12; pp. 375–449.

7. Addiscott, T.M.; Whitmore, A.P.; Powlson, D.S. *Farming, Fertilizers and the Nitrate Problem*; CAB International CABI: Wallingford, UK, 1991; ISBN 0851986587.
8. Wakida, F.T.; Lerner, D.N. Non-agricultural sources of groundwater nitrate: A review and case study. *Water Res.* **2005**, *39*, 3–16. [[CrossRef](#)]
9. Canter, L.W. *Nitrates in Groundwater*; CRC Press Inc.: Boca Raton, FL, USA, 1997.
10. Holloway, J.M.; Dahlgren, R.A. Nitrogen in rock: Occurrences and biogeochemical implications. *Glob. Biogeochem. Cycles* **2002**, *16*, 1118. [[CrossRef](#)]
11. Alfaifi, H.J.; Abdelfatah, M.S.; Abdelrahman, K.; Zaidi, F.K.; Ibrahim, E.; Alarifi, N.S. Groundwater Management Scenarios for the Biyadh-Wasia Aquifer Systems in the Eastern Part of Riyadh Region, Saudi Arabia. *J. Geol. Soc. India* **2017**, *89*, 669–674. [[CrossRef](#)]
12. Ministry of Agriculture and Water (MAW). Water Atlas of Saudi Arabia. In *Ministry of Agriculture and Water in Cooperation with the Saudi Arabian-United States Joint Commission on Economic Cooperation*; MAW: Riyadh, Saudi Arabia, 1984.
13. Al-Omran, A.M.; Aly, A.A.; Al-wabel, M.I. Hydrochemical characterization of groundwater under agricultural land in arid environment: A case study of Al Kharj, Saudi Arabia. *Arab. J. Geosci.* **2016**. [[CrossRef](#)]
14. Zaidi, F.K.; Mogren, S.; Mukhopadhyay, M.; Ibrahim, E. Evaluation of groundwater chemistry and its impact on drinking and irrigation water quality in the eastern part of the Central Arabian graben and trough system, Saudi Arabia. *J. Afr. Earth Sci.* **2016**, *120*, 208–219. [[CrossRef](#)]
15. Alharbi, T.G.; Zaidi, F.K. Hydrochemical classification and multivariate statistical analysis of groundwater from Wadi Sahba area in central Saudi Arabia. *Arab. J. Geosci.* **2018**, *11*, 643. [[CrossRef](#)]
16. GTZ/DCO. *Detailed Water Resources Studies of Wasia-Biyadh and Aruma Aquifers—Groundwater Model and Water Management*; Gesellschaft für Technische Zusammenarbeit, Dornier Consulting, Ministry of Water and Electricity: Riyadh, Saudi Arabia, 2013.
17. GTZ/DCO. *Detailed Water Resources Studies of Wasia-Biyadh and Aruma Aquifers—Phase I Completion Report*; Gesellschaft für Technische Zusammenarbeit, Dornier Consulting, Ministry of Water and Electricity: Riyadh, Saudi Arabia, 2009.
18. Mayer, B.; Boyer, E.W.; Goodale, C.; Jaworski, N.A.; Van Breemen, N.; Howarth, R.W.; Seitzinger, S.; Billen, G.; Lajtha, K.; Nadelhoffer, K. Sources of nitrate in rivers draining sixteen watersheds in the northeastern US: Isotopic constraints. *Biogeochemistry* **2002**, *57*, 171–197. [[CrossRef](#)]
19. Wells, E.R.; Krothe, N.C. Seasonal fluctuation in $\delta^{15}\text{N}$ of groundwater nitrate in a mantled karst aquifer due to macropore transport of fertilizer-derived nitrate. *J. Hydrol.* **1989**, *112*, 191–201. [[CrossRef](#)]
20. Clark, I.D.; Fritz, P. *Environmental Isotopes in Hydrogeology*; CRC press: Boca Raton, FL, USA, 1997.
21. Fetter, C.W. *Applied Hydrogeology*, 4th ed.; Pearson Education, Inc.: Harlow, UK, 2014; ISBN 9781292022901.
22. Almazroui, M. Calibration of TRMM rainfall climatology over Saudi Arabia during 1998–2009. *Atmos. Res.* **2011**, *99*, 400–414. [[CrossRef](#)]
23. Powers, R.W.; Ramirez, L.F.; Redmond, C.D.; Elberg, E.L.J. Geology of the Arabian Peninsula Sedimentary Geology of Saudi Arabia. *U.S. Geol. Surv. Prof. Pap.* **1966**, *560*, 154.
24. Sharief, F.A.; Magara, K.; Abdulla, H.M. Depositional system and reservoir potential of the Middle Cretaceous Wasia Formation in central-eastern Arabia. *Mar. Pet. Geol.* **1989**, *6*, 303–315. [[CrossRef](#)]
25. Keller, M.; Bohnsack, D.; Koch, R.; Hinderer, M.; Hornung, J.; Al-Ajmi, H.; Abu Amarah, B.A. Outcrop Analog Studies of the Wasia-Biyadh and Aruma Aquifers in the Kingdom of Saudi Arabia. In *Siliciclastic Reservoirs of the Arabian Plate*; Al Anzi, H.R., Rahmani, R.A., Steel, R.J., Soliman, O.M., Eds.; AAPG Memoir: Tulsa, OK, USA, 2019; Volume 116, pp. 317–382.
26. BRGM. *Hydrogeological Investigations of the Al Wasia Aquifer in the Eastern Province of Saudi Arabia*; Ministry of Agriculture and Water, Water Resources Development Department: Riyadh, Saudi Arabia, 1976; p. 109.
27. Bazuhair, A.S.A. Optimum Aquifer Yield of Four Aquifers in Al-Kharj Area, Saudi Arabia. *Earth Sci.* **1989**, *2*, 12. [[CrossRef](#)]
28. Edgell, H.S. Aquifers of Saudi Arabia and their geological framework. *Arab. J. Sci. Eng.* **1997**, *22*, 3–31.
29. ARAMCO. *A Study of the Wasia Aquifer in Eastern Saudi Arabia*; Aramco: Riyadh, Saudi Arabia, 1960; p. 128.
30. Birkle, P. Geochemical fingerprinting of hydraulic fracturing fluids from Qusaiba Hot Shale and formation water from Paleozoic petroleum systems, Saudi Arabia. *Geofluids* **2016**, *16*, 565–584. [[CrossRef](#)]

31. GTZ/DCO. *Detailed Water Resources Studies of Wajid and Overlying Aquifers—Environmental Isotopes*; Gesellschaft für Technische Zusammenarbeit, Dornier Consulting, Ministry of Water and Electricity: Riyadh, Saudi Arabia, 2009.
32. McIlvin, M.R.; Altabet, M.A. Chemical conversion of nitrate and nitrite to nitrous oxide for nitrogen and oxygen isotopic analysis in freshwater and seawater. *Anal. Chem.* **2005**, *77*, 5589–5595. [[CrossRef](#)]
33. WHO (World Health Organization). Guidelines for drinking-water quality. *WHO Chron.* **2011**, *4*, 104–108.
34. Michelsen, N.; Reshid, M.; Siebert, C.; Schulz, S.; Knöller, K.; Weise, S.M.; Rausch, R.; Al-Saud, M.; Schüth, C. Isotopic and chemical composition of precipitation in Riyadh, Saudi Arabia. *Chem. Geol.* **2015**, *413*, 51–62. [[CrossRef](#)]
35. Kendall, C.; McDonnell, J.J. *Isotope Tracers in Catchment Hydrology*; Elsevier: Amsterdam, The Netherlands, 1998; p. 839.
36. Vengosh, A.; Heumann, K.G.; Juraske, S.; Kasher, R. Boron isotope application for tracing sources of contamination in groundwater. *Environ. Sci. Technol.* **1994**, *28*, 1968–1974. [[CrossRef](#)]
37. Helvaci, C. Borates. In *Encyclopedia of Geology*; Selley, R.C., Cocks, L.R.M., Plimer, I.R., Eds.; Elsevier: Amsterdam, The Netherlands, 2005; Volume 3, pp. 510–522.
38. WHO. *Guidelines for Drinking-Water Quality*, 4th ed.; Incorporating the First Addendum; WHO: Geneva, Switzerland, 2017; p. 540. ISBN 978-92-4-154995-0.
39. Alabdula'aly, A.I.; Khan, M.A. Chemistry of rain water in Riyadh, Saudi Arabia. *Arch. Environ. Contam. Toxicol.* **2000**, *39*, 66–73. [[CrossRef](#)] [[PubMed](#)]
40. Meiklejohn, B.Y.J. Iron and the Nitrifying Bacteria. *Microbiology* **1953**, *8*, 58–65. [[CrossRef](#)] [[PubMed](#)]
41. Qian, G.; Hu, X.; Li, L.; Ye, L.; Lv, W. Effect of iron ions and electric field on nitrification process in the periodic reversal bioelectrocoagulation system. *Bioresour. Technol.* **2017**, *244*, 382–390. [[CrossRef](#)] [[PubMed](#)]
42. Le Nindre, Y.M.; Vaslet, D.; Maddah, S.S.; Al-Husseini, M.I. Stratigraphy of the Valanginian? To early Paleocene succession in central Saudi Arabia outcrops: Implications for regional Arabian sequence stratigraphy. *GeoArabia* **2008**, *13*, 51–86.
43. Keeney, D.; Olson, R.A. *Sources of Nitrate to Ground Water*; Taylor & Francis: Abingdon-on-Thames, UK; London, UK, 1986; Volume 16, ISBN 1064338860.
44. Alabdula'aly, A.; Al-Rehaili, A.M.; Al-Zarah, A.I.; Khan, M.A. Assessment of nitrate concentration in groundwater in Saudi Arabia. *Environ. Monit. Assess.* **2010**, *161*, 1–9. [[CrossRef](#)] [[PubMed](#)]
45. Al-Mutaz, I.S. Water resources development in Riyadh, Saudi Arabia. *Desalination* **1987**, *64*, 193–202. [[CrossRef](#)]



© 2020 by the authors. Licensee MDPI, Basel, Switzerland. This article is an open access article distributed under the terms and conditions of the Creative Commons Attribution (CC BY) license (<http://creativecommons.org/licenses/by/4.0/>).